IOPscience iopscience.iop.org

Home Search Collections Journals About Contact us My IOPscience

The use of a Ga^{+} focused ion beam to modify graphene for device applications

This article has been downloaded from IOPscience. Please scroll down to see the full text article.

2012 Nanotechnology 23 255305

(http://iopscience.iop.org/0957-4484/23/25/255305)

View the table of contents for this issue, or go to the journal homepage for more

Download details:
IP Address: 200.130.18.1
The article was downloaded on 10/07/2012 at 03:55

Please note that terms and conditions apply.

Nanotechnology **23** (2012) 255305 (6pp) doi:10.1088/0957-4484/23/25/255305

The use of a Ga^+ focused ion beam to modify graphene for device applications

B S Archanjo[1], A P M Barboza[2], B R A Neves[2], L M Malard[2], E H M Ferreira[1], J C Brant[2], E S Alves[2], F Plentz[2], V Carozo[1], B Fragneaud[1], I O Maciel[3], C M Almeida[1], A Jorio[2] and C A Achete[1,4]

[1] Divisão de Metrologia de Materiais, Instituto Nacional de Metrologia, Normalização e Qualidade Industrial, Duque de Caxias, RJ, 25250-020, Brazil
[2] Departamento de Física, Universidade Federal de Minas Gerais, Belo Horizonte, MG, 30123-970, Brazil
[3] Departamento de Física, Instituto de Ciências Exatas, Universidade Federal de Juiz de Fora, 36036-330 Juiz de Fora, MG, Brazil
[4] Programa de Engenharia Metalúrgica e de Materiais (PEMM), Universidade Federal do Rio de Janeiro, Caixo Postal 68505, CEP 21945-970, Rio de Janeiro, RJ, Brazil

E-mail: bsarchanjo@inmetro.gov.br

Received 27 February 2012, in final form 25 April 2012
Published 31 May 2012
Online at stacks.iop.org/Nano/23/255305

Abstract
In this work, we clarify the features of the lateral damage of line defects in single layer graphene. The line defects were produced through well-controlled etching of graphene using a Ga^+ focused ion beam. The lateral damage length was obtained from both the integrated intensity of the disorder induced Raman D band and the minimum ion fluence. Also, the line defects were characterized by polarized Raman spectroscopy. It was found that graphene is resilient under the etching conditions since the intensity of the defect induced Raman D peak exhibits a dependence on the direction of the lines relative to the crystalline lattice and also on the direction of the laser polarization relative to the lines. In addition, electrical measurements of the modified graphene were performed. Different ion fluences were used in order to obtain a completely insulating defect line in graphene, which was determined experimentally by means of charge injection and electric force microscopy measurements. These studies demonstrate that a Ga+ ion column combined with Raman spectroscopy is a powerful technique to produce and understand well-defined periodic arrays of defects in graphene, opening possibilities for better control of nanocarbon devices.

(Some figures may appear in colour only in the online journal)

1. Introduction

Graphene, a two-dimensional carbon structure, is a model system that comprises exciting possibilities to demonstrate new physics and novel electronic applications [1–3], many of which can be appreciated only by means of nanoscale modifications to its structure [4, 5]. The study of defects, impurities and spatial confinement in single layer graphene is of great importance for understanding the behavior of this material and also tuning its properties for different applications [4, 6, 7]. Graphene samples produced via mechanical exfoliation have sizes in the range of ∼5 nm up to the micrometer scale. Some promising applications can be found in ballistic room-temperature transistors [8–10], carbon-based spintronic devices [11, 12], and permeation membranes [13]. Graphene nanostructures have already been fabricated by electron beam lithography followed by reactive ion etching [14–20], scanning tunneling microscopy lithography [21], atomic force microscopy anodic oxidation [22], and chemically derived techniques [23, 24]. Further modification of these structures is mainly performed by electron and ion radiation [25, 26] where focused ion beams have the advantage of achieving well-controlled modification at the nanometer scale [25, 27, 28].

 © 2012 IOP Publishing Ltd Printed in the UK & the USA

Raman spectroscopy (RS) is one of the most used techniques to probe the presence of defects and even to quantify the amount of disorder generated by ion implantation on graphitic materials [7, 25, 29–33]. The first order Raman spectrum of any sp^2 carbon material is comprised by one peak around 1580 cm^{-1}, called the G band, which is related to the in-plane stretching mode of the C–C bonds [29]. However, when there is a symmetry breaking in the graphene lattice due to the presence of a defect such as a vacancy or an edge, it is possible to observe two new features around 1360 cm^{-1} and 1620 cm^{-1}, called D and D′ bands, respectively. The ratio between the intensities of the D and G bands (I_D/I_G) is commonly used to monitor the density of defects [29]. The D band intensity also depends on the atomic structure of the edges as well as on the laser polarization direction related to the edge: the D band is stronger for polarization parallel to the edge and minimum for the perpendicular direction. In the case of an ideal edge, when the polarization is perpendicular to the border, the D peak intensity is weaker for zigzag orientation and stronger for armchair orientation [34, 35].

In this work we use a dual beam microscope equipped with a focused Ga^+ ion beam source (FIB source) with an electron field emission gun (FEG) to modify single layer graphene samples. The modifications are further characterized using Raman spectroscopy, electrical measurements (EMs), electric force microscopy (EFM) and atomic force microscopy (AFM). Full characterization of the use of FIB for graphene patterning is presented, allowing the determination of the minimum ion dose that generates an insulating line in a graphene single layer. Spectroscopic and electrical measurements of the behavior of a periodical array of lines generated by Ga^+ FIB in a low fluence are investigated. Our motivation relies on proving suitable characteristics of Ga^+ FIB sources. This is a well established commercial technique accessible to many laboratories and, in addition, there is no need to deposit and remove materials as one frequently does in lithography related techniques.

2. Experimental details

The graphene samples used here were deposited on Si wafers with a 300 nm SiO_2 top layer by a mechanical exfoliation technique as described in [2]. The samples were localized with an optical microscope and the numbers of layers were identified by both Raman spectroscopy [36] and AFM. The ion bombardment and the FEG-SEM images were performed using respectively a Nova Nanolab dual beam platform and a Magellan 400, both from FEI Company, where the SEM images were acquired using a 1 keV accelerating energy and a 13 pA electron current. For the ion bombardment, a two-lens UHV magnum Ga^+ ion column working at 30 keV accelerating energy was used, with an ion current of about 0.8 pA and different dwell times (writing speeds), which could go down to 100 ns per dot providing 5–7 nm final resolution. A Nanoscope IV MultiMode SPM, from Veeco Instruments, and a Nano Wizard AFM (JPK) were employed for structural and morphological analysis. SPM measurements were carried out in air or under dry nitrogen atmosphere with the help of homemade environmental control chambers. Gold-covered silicon cantilevers with nominal spring constant of $k \sim$ 0.25–2 N m^{-1}, nominal curvature radius of $R \sim 25$ nm and resonant frequency of $\omega_0 \sim$ 20–80 kHz were employed for atomic force microscopy (AFM) imaging (intermittent contact mode) and EFM (electric force microscopy) experiments. More accurate estimations of k and R were carried out by using Sader's method [37] and by imaging reference samples, respectively. The micro-Raman images and spectra were acquired using a Witec Alpha300 AR atomic force and confocal Raman microscopy system with an excitation energy of 2.33 eV (532 nm) and a Jobin Yvon T64000 spectrometer in backscattering configuration with an excitation energy of 2.41 eV (514.5 nm).

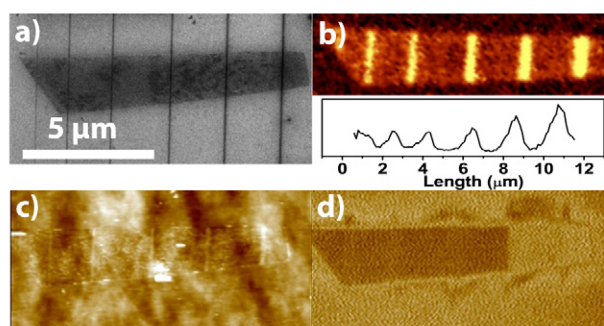

Figure 1. A graphene single layer with six bombarded lines using different ion doses. The dose increases from left to right. (a) SEM image. (b) Top: Raman map of the integrated intensity of the D band. Bottom: line profile of the Raman map. (c) AFM image of the sample topography. (d) Electric force microscopy image of the graphene sample after charging, showing that there is no charge after the fifth line ($V = 1$ V, lift height $= 50$ nm).

3. Results and discussion

In order to modify graphene-based devices in a controlled way, one of the first steps is to determine the ion dose for which the graphene sheet can have a totally insulating line, as well as the lateral damaged area for different ion doses. In order to do that, we made linear patterns with different ion doses in a single layer graphene sample, as shown in figure 1(a). Each line was formed by a set of 10 nm spots. The beam stayed in each spot for a controlled time (dwell time), which was related to the writing speed of the bombardment. The dwell time was changed from 1 μs up to 1 ms (from left to right in figure 1(a)), and the ion dose was varied from 6×10^{12} to 6×10^{15} ions cm^{-2} accordingly. Table 1 shows the dwell time, ion dose and lateral profile for each line made in the graphene sample. The dwell time, and consequently the ion dose, was increased from left to right and, as expected, a higher dose led to a broader line, as can been seen from the two-dimensional map of Raman D peak intensity shown in figure 1(b). The lateral damage was obtained from the profile depicted in the bottom part of figure 1(b) as discussed below.

To address the problem of the minimum dose necessary to generate an insulating line, we performed charge injection

Table 1. A summary of FIB dwell time, ion dose and lateral line width taken from different techniques for each bombarded line.

Line	1	2	3	4	5	6
Dwell time (μs)	1	10	50	100	500	1000
Dose (ions cm^{-2})	6×10^{12}	6×10^{13}	3×10^{14}	6×10^{14}	3×10^{15}	6×10^{15}
Profile width[a] (nm)	23 ± 2	35 ± 4	40 ± 4	40 ± 4	49 ± 5	72 ± 7
Profile width[b] (μm)	0.65 ± 0.06	0.65 ± 0.06	0.68 ± 0.07	0.63 ± 0.06	0.74 ± 0.07	1.0 ± 0.1

[a] Profile width obtained directly from the SEM image.

[b] Profile width obtained from the profile plot in figure 1(b).

experiments using EFM. The graphene slice was charged through contact with a properly biased AFM tip in a dry atmosphere [38]. No bias was applied between the tip and the sample during the second pass (EFM) imaging after charge injection. The extra charges injected in the sample induced image charges of opposite sign in the EFM tip during the second pass, leading to an attractive tip–sample interaction which shifted the cantilever oscillation frequency to a lower value. Figures 1(c) and (d) show the AFM and EFM images, respectively. In the sequence, a bias of 1 V was applied at the AFM tip, which generated charge injection in the left side of the sample. As shown in figure 1(d), no charge was transferred through the fifth line. Hence, as shown in table 1, we find that 3×10^{15} ions cm^{-2} is the minimum dose needed to create an insulating edge in the graphene layer.

In general, the experimentally determined values for a-C:H sputter yield for Ga^+ ion sources working at 30 kV fall between 2.3 and 2.8 carbon atoms per incident ion. However, theoretical models such as transport of ions in matter (TRIM) or linear cascade collision (LCC) indicate values for carbon sputter yield in the range of 1.2–1.7 [39]. On the other hand, due to its two-dimensional character, graphene has presented experimentally determined yield values between 0.3 and 0.4 for Ga^+ ion sources working at 30 kV [39]. Furthermore, theoretical calculations for suspended graphene [40, 41] show that 35% of the carbon atoms are removed leading to an amorphization level of 95% using a 3×10^{15} ions cm^{-2} dose. For a two times higher dose, (experimental results shown in the sixth line of table 1), the simulation predicts about 56% of removed carbon atoms and almost 99% of amorphization. Given that a single layer of graphene has 3.8×10^{15} carbon atoms cm^{-2}, and since the dose of the fifth line (table 1) is enough to create an insulating line, we conclude that one Ga^+ ion at 30 keV per carbon atom is enough to generate a sufficient amount of defects in order to obtain an insulating carbon layer. Therefore, we conclude that it is not necessary to remove all carbon atoms to create an insulating structure inside a single layer of graphene. This is actually expected since other types of defect such as amorphization and foreign and carbon adatoms have a strong influence on the electrical conductivity. Such adatoms come from the atmosphere inside the FIB chamber, the substrate, and impurities on the graphene layer. In addition, the effect of the substrate substantially increases the damage probability by enlarging the damaged width due to plastic deformation for low fluence and amorphization and sputtering for high fluence. By taking into account that the graphene amorphization is substantially enhanced by these impurities and the substrate, we conclude that both experimental [39] and theoretical [40, 41] results are in good agreement with our experiment.

In [42] we showed that Raman spectroscopy is the most sensitive technique as it is able to measure the effects of ion bombardment in graphite structure for fluences down to 10^{11} ions cm^{-2}. Therefore, we used this suitable sensitivity to obtain the lateral damaged width of a bombarded line and compared it to the line width directly obtained from the SEM image (table 1). Therefore we analyzed the intensity profile of the D peak across the defect lines. Since the four first lines have a width ($\leq$40 nm from table 1) much smaller than the laser focus diameter, the D band intensity profile obtained from these lines was used in order to estimate the intensity profile (point spread function) of the incident laser line used in the Raman experiments. By deconvoluting the D band response and the point spread function of the incident laser from the D band intensity profile, we were able to estimate the lateral damaged widths in the fifth and sixth lines as 90 ± 20 nm and 350 ± 70 nm, respectively. Although the FIB diameter is expected to have nominally 7 nm, the smaller measured line width obtained from the SEM image is about 23 nm. Besides, from the fifth to sixth lines the lateral damaged width increases significantly when comparing the SEM line width, showing that the influence of the experimental parameters such as imperfect high vacuum and impurities due to backscattered atoms from the substrate play an important role in the study of sharpness of an edge produced via focused ion beam bombardment in single layer graphene. In the case of the highest dose used here (6×10^{15} ions cm^{-2}) which, according the [39], is close to the dose needed to completely remove the graphene layer, we show that we have a line width (extracted from the SEM image) of 72 ± 7 nm and a lateral damaged width of 350 ± 70 nm. This is an important result for the development of graphene nanostructures using Ga^+ FIB, since it shows that one must consider this lateral damaged width in order to obtain the correct shape when making an insulating region or completely removing graphene areas.

In order to study defects at low modification levels, we generated patterns using ion doses lower than 6×10^{13} ions cm^{-2}. For such low fluence, previous theoretical studies [40, 41] predict 1% of lost atoms and 6% amorphization in the graphene structure inside the bombarded line. We have created patterns with parallel lines on a single layer of graphene, obtaining a periodic structure as shown in figures 2(a) and (b). This new bombardment configuration allowed us to have a better understanding about the structural

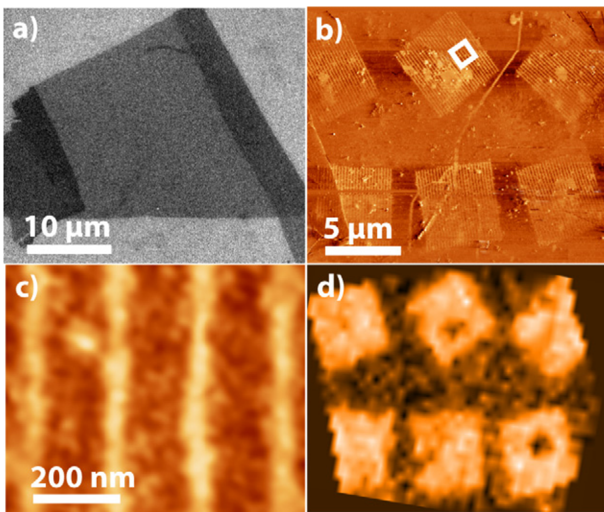

Figure 2. (a) SEM image and (b) atomic force microscopy phase image showing a graphene single layer with square patterns having bombarded lines at different orientations spaced by 200 nm. (c) Higher magnification of a selected area of (b). (d) Raman map of the integrated intensity of the D band.

damage via polarized Raman spectroscopy analysis. The bombarded sample was analyzed by atomic force microscopy and polarized micro-Raman spectroscopy in order to verify the amount of defects created. In figure 2(a) we show an SEM image of single layer graphene on a silicon dioxide substrate. The darker shades on the left and right sides of the flake indicate the presence of more than one layer in these regions. The brighter part in the middle is a large area ($\sim$500 μm^2) where single layer graphene is present. We performed the ion bombardment with patterned lines spaced from each other by 200 nm inside a square of 5 $\times$ 5 μm^2. All six squares patterned in the sample were rotated by 10° relative to their respective neighbor, as can be seen from figure 2(b) where an AFM phase image is shown. Figure 2(c) is a magnified view of the region marked by a white square in figure 2(b). In this magnified phase image one can see that the lines have a width of around 30 nm, which is in agreement with results from our previous work [42] showing the topographic changes due to single bombarded spots. This image also reveals that the lines are well defined, suggesting that only a small amount of ions may fall outside the patterned lines. After ion bombardment, the sample was baked in argon atmosphere for 24 h at 400 °C in order to remove amorphous carbon deposited during the bombardment process, or adatoms physically adsorbed during the manipulation inside the electron microscope chamber. The micro-Raman maps of the integrated intensity of the D band can be seen in figure 2(d). It can be seen from D band map that the defects are concentrated in the specific bombarded area and almost no defects are found outside this area, showing that an FIB can pattern a specific area of a device without generating considerable damage in neighboring regions.

In order to study the spatial spreading and orientation of the defects in the patterned lines the polarization of the incident laser during micro-Raman experiments was changed [34, 35]. The Raman spectra of the graphene sheet for the laser polarization parallel and perpendicular to the patterned lines of one of the squares can be seen in figure 3(a). The intensity ratios I_D/I_G are slightly different for parallel and perpendicular laser polarization, suggesting that the patterned lines may present edge behavior. Theoretically, we would expect that a perfect armchair (zigzag) graphene edge would show a stronger (null) D band when the incident laser polarization was parallel to it [34, 35]. In figure 3(b) we show the Raman spectra with incident light polarization parallel to the edges of two different squares, which in turn are rotated by 20° from each other. As depicted in the graphics, different intensity ratios are observed, showing that the bottom right pattern has a higher percentage of armchair sites than the bottom left pattern. However, the polarization effect is rather weak and we believe it can be improved in future experiments by using a higher resolution ion source.

To show the applicability of an FIB in generating periodical defects in graphene we used a graphene Hall bar and studied the changes in the electrical properties of a bombarded area. The Hall bar shown in figure 4(a) was built by electron beam lithography with the materials and methods discussed in a previous work [20]. The bombardment was performed using the same ion current as before with a dwell time of 6 μs or a spot dose of 4 $\times$ 10^{13} ions cm^{-2} (approximately 30 ions per dot). The pattern was a periodical array of lines spaced by 80 nm with the lines perpendicular to the direction of current flow. In figure 4(a) the white square highlights the bombarded area. In figures 4(b) and

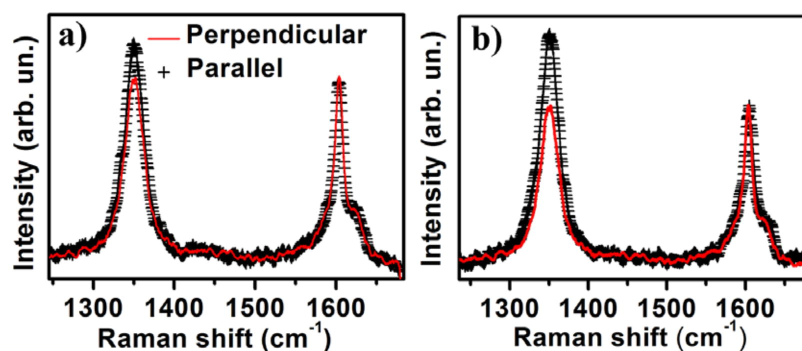

Figure 3. Raman spectra showing D and G bands (a) for parallel and perpendicular laser polarizations for one set of parallel lines and (b) for parallel laser polarization at two different sets of parallel lines rotated by 20°.

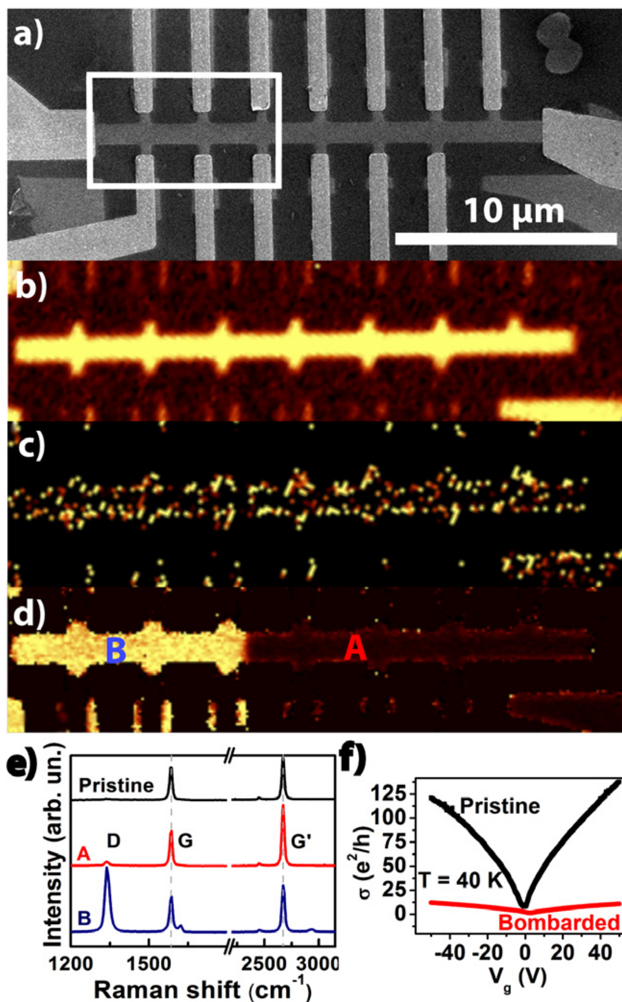

Figure 4. (a) SEM image showing a graphene Hall bar built using electron beam lithography. (b)–(d) Raman maps of the integrated intensities of (b) the G band before bombardment, (c) the D band before bombardment and (d) the D band after ion bombardment. (e) Plots contrasting the differences in Raman spectra of the pristine, non-bombarded (point A in (d)) and bombarded (point B in (d)) regions. (f) Conductivity versus gate voltage of the pristine and bombarded regions.

(c), we respectively show two-dimensional maps of Raman G and D peak intensities prior to the ion bombardment. The image in figure 4(c) demonstrates the good quality of the graphene layer even after the lift-off process, since there are defects only in the etched borders. In figure 4(d) we show a two-dimensional map of Raman D peak intensity of the same device after ion bombardment confirming that the defective area is on the left side as it was intended in the ion bombardment blind step. Analyzing the Raman spectra of pristine (before bombardment), bombarded and non-bombarded regions in figure 4(e), we see that no shifts are observed in the Raman bands. However, after ion exposure even the non-bombarded region presents a low intensity D band. We believe that this small amount of defects is due to electron beam imaging and some unwanted non-focused ions, showing how sensitive single layer graphene is to such procedures. Comparing the conductivity versus gate voltage (figure 4(f)) of the bombarded graphene and non-bombarded graphene, we observe a general trend of decrease in conductivity after bombardment. These results agree with other works where the bombarded pattern was not periodical [43–45]. They show that the defects decrease the mobility of the sample and also cause a shift of the Fermi level which is related to doping, shifting the position of the Dirac point to positive values. Using only $\sigma V_g \sigma = \mu e \alpha V_g$, where σ is the conductivity, μ is the mobility, e is the electron charge, $\alpha = 7.2 \times 10^{10}$ cm^{-2} V^{-1} is a constant found from the device gate capacitance and V_g is the gate voltage, it can be seen, though, that the σV_g measured curves are sublinear. Therefore, to extract the mobility, we linearized the curves using a procedure described by Morozov *et al* [46] and then we made the linear fit. Using this method we extracted mobilities of 1200 cm^2 V^{-1} s^{-1} for the pristine part of the device and 120 cm^2 V^{-1} s^{-1} for the irradiated part of the device.

Currently we are further investigating the effect of the periodicity of the bombardment pattern on the electrical behavior of graphene.

4. Conclusions

Using the Ga^+ FIB technique, we generated defects along lines and periodic arrays of lines on single layer graphene. We studied the morphological, electrical and optical properties of the graphene area affected by the defects, demonstrating the accuracy of an FIB in patterning and creating defects in single layer graphene, and showing that this tool can be applied in building and modifying graphene nanodevices. We have shown that the size of the lateral damaged area generated by an FIB is an important parameter that determines whether the defect forms an electrical insulating line or not. For lines created with a low fluence, we observed interesting properties in polarized micro-Raman experiments, showing that defects along lines behave similarly to graphene edges, opening new possibilities in generating and analyzing periodic defects at the nanoscale range. We have also shown an electrical measurement in order to exemplify the applicability of an FIB in changing the electrical properties of a graphene device. In short, we demonstrate in this study that the direct writing of patterns on graphene via Ga^+ FIB can provide new results in graphene-based electronics.

Acknowledgments

The authors sincerely thank Professor Luiz Gustavo Cançado for carefully reading the manuscript and also acknowledge the financial support from the Brazilian Agencies CNPq, FINEP, FAPERJ and FAPEMIG.

References

[1] Novoselov K S, Geim A K, Morozov S V, Jiang D, Zhang Y, Dubonos S V, Grigorieva I V and Firsov A A 2004 Electric field effect in atomically thin carbon films *Science* **306** 666

[2] Geim A K and Novoselov K S 2007 The rise of graphene *Nature Mater.* **6** 183

[3] Noorden R V 2006 Moving towards a graphene world *Nature* **442** 228
[4] Park C H, Yang L, Son Y W, Cohen M L and Louie S G 2008 *Nature Phys.* **4** 213
[5] La Magna A, Deretzis I, Forte G and Pucci R 2009 Conductance distribution in doped and defected graphene nanoribbons *Phys. Rev.* B **80** 195413
[6] Terrones M *et al* 2010 Graphene and graphite nanoribbons: morphology, properties, synthesis, defects and applications *Nano Today* **5** 351
[7] Lucchese M M, Stavale F, Ferreira E H M, Vilani C, Moutinho M V O, Capaz R B, Achete C A and Jorio A 2010 Quantifying ion-induced defects and Raman relaxation length in graphene by Raman spectroscopy *Carbon* **48** 1592
[8] Obradovic B, Kotlyar R, Heinz F, Matagne P, Rakshit T, Giles M D, Stettler M A and Nikonov D E 2006 Analysis of graphene nanoribbons as a channel material for field-effect transistors *Appl. Phys. Lett.* **88** 142102
[9] Areshkin D A, Gunlycke D and White C T 2007 Ballistic transport in graphene nanostrips in the presence of disorder: importance of edge effects *Nano Lett.* **7** 204
[10] Liang G C, Neophytou N, Nikonov D E and andd Lundstrom M S 2007 Performance projections for ballistic graphene nanoribbon field-effect transistors *IEEE Trans. Electron Devices* **54** 677
[11] Son Y W, Cohen M L and Louie S G 2006 Half-metallic graphene nanoribbons *Nature* **444** 347
[12] Wang W L, Meng S and Kaxiras E 2008 Graphene nanoflakes with large spin *Nano Lett.* **8** 241
[13] Bayley H 2010 Holes with an edge *Nature* **467** 164
[14] Han M Y, Ozylimaz B, Zhang Y and Kim P 2007 Energy band-gap engineering of graphene nanoribbons *Phys. Rev. Lett.* **98** 206805
[15] Heydrich S, Hirmer M, Preis C, Korn T, Eroms J, Weiss D and Schüller C 2010 Scanning Raman spectroscopy of graphene antidot lattices: evidence for systematic p-type doping *Appl. Phys. Lett.* **97** 043113
[16] Chen Z, Lin Y M, Rooks M J and Avouris P 2007 Graphene nano-ribbon electronics *Physica* E **40** 228
[17] Ponomarenko L A, Schedin F, Katsnelson M I, Yang R, Hill E W, Novoselov K S and Geim A K 2008 Chaotic Dirac billard in graphene quantum dots *Science* **320** 356
[18] Stampfer C, Güttinger J, Molitor F, Graf D, Ihn T and Ensslin K 2008 Tunable Coulomb blockade in nanostructured graphene *Appl. Phys. Lett.* **92** 012102
[19] Ozyilmaz B, Jarillo-Herrero P, Efetov D and Kim P 2007 Electronic transport in locally gated graphene nanoconstrictions *Appl. Phys. Lett.* **91** 192107
[20] Brant J C, Leon J, Barbosa T C, Araujo E N D, Archanjo B S, Plentz F and Alves E S 2010 Hysteresis in the resistance of a graphene device induced by charge modulation in the substrate *Appl. Phys. Lett.* **97** 042113
[21] Tapaszto L, Dobrik G, Lambin P and Biro L P 2008 Tailoring the atomic structure of graphene nanoribbons by scanning tunnelling microscope lithography *Nature Nanotechnol.* **3** 397
[22] Masubuchi S O M, Yoshida K, Hirakawa K and Machida T 2009 Fabrication of graphene nanoribbon by local anodic oxidation lithography using atomic force microscope *Appl. Phys. Lett.* **94** 082107
[23] Li X L, Wang X R, Zhang L, Lee S W and Dai H J 2008 Chemically derived, ultrasmooth graphene nanoribbon semiconductors *Science* **319** 1229
[24] Campos L C, Manfrinato V R, Sanchez-Yamagishi J D, Kong J and Jarillo-Herrero P 2009 Anisotropic etching and nanoribbon formation in single-layer graphene *Nano Lett.* **9** 2600
[25] Krasheninnikov A V and Nordlund K 2010 Ion and electron irradiation-induced effects in nanostructured materials *J. Appl. Phys.* **107** 071301
[26] Teweldebrhan D and Balandina A A 2009 Modification of graphene properties due to electron-beam irradiation *Appl. Phys. Lett.* **94** 013101
[27] Park C H, Yang L, Son Y W, Cohen M L and Louie S G 2008 Anisotropic behaviours of massless Dirac fermions in graphene under periodic potentials *Nature Phys.* **4** 213
[28] Bella D C, Lemme M C, Stern L A and Marcus C M 2009 Precision material modification and patterning with He ions *J. Vac. Sci. Technol.* B **27** 2756
[29] Dresselhaus M S and Kalish R 1992 *Ion Implantation in Diamond, Graphite and Related Materials* (Berlin: Springer)
[30] Tuinstra F and Koenig J L 1970 Raman spectrum of graphite *J. Chem. Phys.* **53** 1126
[31] Ferrari A C and Robertson J 2000 Interpretation of Raman spectra of disordered and amorphous carbon *Phys. Rev.* B **61** 14095
[32] Jorio A, Lucchese M M, Stavale F and Achete C A 2009 Raman spectroscopy study of Ar^+ bombardment in highly oriented pyrolytic graphite *Phys. Status Solidi* B **246** 2689
[33] Nakamura K and Kitajima M 1992 Ion-irradiation effects on the phonon correlation length of graphite studies by raman-spectroscopy *Phys. Rev.* B **45** 78
[34] Cancado L G, Pimenta M A, Neves B R A, Dantas M S S and Jorio A 2004 Influence of the atomic structure on the Raman spectra of graphite *Phys. Rev. Lett.* **93** 247401
[35] Casiraghi C, Hartschuh A, Qian H, Piscanec S, Georgi C, Fasoli A, Novoselov K S, Basko D M and Ferrari A C 2009 Raman spectroscopy of graphene edges *Nano Lett.* **9** 1433
[36] Ferrari A C *et al* 2006 Raman spectrum of graphene and graphene Layers *Phys. Rev. Lett.* **97** 187401
[37] Sader J E, Chon J W M and Mulvaney P 1999 Calibration of rectangular atomic force microscope cantilevers *Rev. Sci. Instrum.* **70** 3067
[38] Barboza A P M, Guimaraes M H D, Massote D V P, Campos L C, Barbosa Neto N M, Cancado L G, Lacerda R G, Chacham H, Mazzoni M S C and Neves B R A 2011 Room-temperature compression-induced diamondization of few-layer graphene *Adv. Mater.* **23** 3014
[39] Lopez J J, Greer F and Greer J R 2010 Enhanced resistance of single-layer graphene to ion bombardment *J. Appl. Phys.* **107** 104326
[40] Lehtinen O, Kotakoski J, Krasheninnikov A V, Tolvanen A, Nordlund K and Keinonen J 2010 Effects of ion bombardment on a two-dimensional target: atomistic simulations of graphene irradiation *Phys. Rev.* B **81** 153401
[41] Lehtinen O, Kotakoski J, Krasheninnikov A V and Keinonen J 2011 Cutting and controlled modification of graphene with ion beams *Nanotechnology* **22** 175306
[42] Archanjo B S, Maciel I O, Ferreira E H M, Peripolli S B, Damasceno J C, Achete C A and Jorio A 2011 Ion beam nanopatterning and micro-Raman spectroscopy analysis on HOPG for testing FIB performances *Ultramicroscopy* **111** 1338
[43] Chen J H, Cullen W G, Jang C, Fuhrer M S and Williams E D 2009 Defect scattering in graphene *Phys. Rev. Lett.* **102** 236805
[44] Zhou Y B, Liao Z M, Wang Y F, Duesberg G S, Xu J, Fu Q, Wu X S and Yu D P 2010 Ion irradiation induced structural and electrical transition in graphene *J. Chem. Phys.* **133** 234703
[45] Lucot D, Gierak J, Ouerghi A, Bourhis E, Faini G and Mailly D 2009 Deposition and FIB direct patterning of nanowires and nanorings into suspended sheets of graphene *Microelectron. Eng.* **86** 882
[46] Morozov S V, Novoselov K S, Katsnelson M I, Schedin F, Elias D C, Jaszczak J A and Geim A K 2008 Giant intrinsic carrier mobilities in graphene and its bilayer *Phys. Rev. Lett.* **100** 016602